Thermomechanical Properties of TiNi Shape Memory Alloy

H. Tobushi, A. Ikai, S. Yamada, K. Tanaka, C. Lexcellent

JOURNAL DE PHYSIQUE IV
Colloque C1, supplément au Journal de Physique III, Volume 6, janvier 1996

Thermomechanical Properties of TiNi Shape Memory Alloy

H. Tobushi, A. Ikai*, S. Yamada**, K. Tanaka*** and C. Lexcellent****

Department of Mechanical Engineering, Aichi Institute of Technology, 1247 Yachigusa, Yagusa-cho, Toyota 470-03, Japan
** Rinnai Co., Ltd., 2-26 Fukuzumi-cho, Nakagawa-ku, Nagoya 454, Japan*
*** Graduate School, Aichi Institute of Technology, Japan*
**** Department of Aerospace Engineering, Tokyo Metropolitan Institute of Technology, 6-6 Asahigaoka, Hino, Tokyo 191, Japan*
***** Laboratoire de Mécanique Appliquée, Université de Franche-Comté, Route de Gray, La Bouloie, 25030 Besançon, France*

Abstract

The thermomechanical properties of shape memory effect and superelasticity due to the martensitic transformation and the R-phase transformation of TiNi shape memory alloy were investigated experimentally. The transformation line, recovery stress and fatigue property due to both transformations were discussed for cyclic deformation. The thermomechanical properties due to the R-phase transformation were excellent for deformation with high cycles.

1. INTRODUCTION

In shape memory alloy (SMA), shape memory effect (SME) and superelasticity (SE) or transformation pseudoelasticity appear depending on stress and temperature. In TiNi SMA, SME and SE appear due to the martensitic transformation (MT) and the rhombohedral phase transformation (RPT) [1]-[3].

In the applications to an actuator, a robot and a solid-state heat engine, SMA is used as a working element which performs cyclic motions. The working characteristics of the SMA element are specified by the beginning and completion temperatures of the motion, the working stroke and the working force. These characteristic values are determined by the transformation temperature, the transformation strain and the transformation stress. The characteristic values associated with the transformation vary through cyclic deformation [4], and fatigue occurs under deformation with high cycles [5][6]. Thus to design the SMA element, the behavior of the above-mentioned characteristic values subjected to thermomechanical cycles becomes crucial.

In the current study, the thermomechanical properties of TiNi SMA associated with MT and RPT, such as SME, SE, transformation line, recovery stress and fatigue are discussed on a wire and a helical spring.

2. EXPERIMENTAL METHOD

2.1 Materials and specimen

The material was a Ti-55.3wt%Ni SMA wire, 0.75mm in diameter. The specimens were given shape memory of a straight line and a helical spring through shape memory processing. This was done by holding the wire in the desired shape at 673K for 60min and cooling in the furnace. The pitch of the helical spring was 2.2mm, the mean spring diameter 9mm, the number of active coil turns $8 \sim 18$. The reverse transformation completion temperature A_f was about 323K which was determined by tensile test. Transformation temperatures determined by DSC were as follows : M_s = 247K, M_f = 199K, A_s = 294K, A_f = 333K for MT and M_s' = 325K, M_f' = 311K, A_s' = 315K, A_f' = 333K for RPT.

2.2 Experimental apparatus

The experimental apparatus used for testing SME and SE of the wire was a shape memory property testing machine [7]. The testing machine was composed of a tensile machine and a heating-cooling device. The specimen was heated by hot air or cooled by liquified carbon dioxide. The gauge length of an extensometer was 20mm.

The experimental apparatus used for testing recovery force of the helical spring was an offset-crank SMA heat engine [8]. In the heat engine the SMA helical springs were mounted on the circumferences of a large disk and a small disk that were eccentric. The heating part was immersed in hot water and cooling part was in air.

The experimental apparatus used for testing fatigue of the wire was a rotating-bending fatigue testing device. The specimen bent in a certain curvature was rotated in a chamber at a constant temperature.

2.3 Experimental procedure

To investigate the thermomechanical properties, the following five experiments were carried out.

(1) Test for SME

In the experiment, the cyclic properties of SME were examined for the wire [9]. At first, the loading and unloading processes with maximum strain ε_m were performed at the low temperature T_l below A_s. Maintaining load zero, the process of heating was performed to the high temperature T_h above A_f followed by cooling to T_l. These loading-unloading and heating-cooling processes were repeated.

(2) Test for SE

In the experiment, the cyclic properties of SE were examined for the wire [10]. The loading and unloading processes were repeated at temperature T above A_f for the maximum strain ε_m.

(3) Test for recovery stress of wire

In the experiment, the cyclic properties of recovery stress of the wire were examined [11]. At first, the loading and unloading processes with maximum strain ε_m were performed at the low temperature T_l below A_s. Holding residual strain constant, the specimen was heated to the high temperature T_h above A_f followed by cooling to T_l. The heating-cooling process was repeated.

(4) Test for recovery force of helical spring

The experiments were performed with no load and the rotational speed was about 65rpm [12]. In each cycle the helical spring was subjected to the maximum and minimum elongations for each number of coil turns. By detaching SMA coils from the heat engine at the prescribed number of cycles, the axial force under the maximum deflection were measured in hot water and in air.

(5) Test for fatigue

The rotating-bending test was performed with no load at the constant temperature and the rotational speed was 500rpm [13]. The number of cycles to failure was measured for each strain amplitude ε_a which was the maximum bending strain on the surface of the wire.

3. EXPERIMENTAL RESULTS AND DISCUSSION

3.1 Shape memory effect

3.1.1 SME due to RPT

The stress-strain curves obtained by the experiments for maximum strain ε_m of 1% are shown in Fig.1 and the corresponding strain-temperature curves are shown in Fig.2. The curves are parametrized by the number of cycles N. As seen in Fig.1, yielding due to RPT occurs under stress of 60MPa in the loading process and residual strain of 0.6% appears after unloading. As seen in Fig.2, strain recovers due to the reverse transformation in the heating process, showing SME. Strain is almost zero in the cooling process. The stress-strain curves and the strain-temperature curves vary little in N=1～10. Thus it is ascertained that the property of SME associated with RPT is stable for cyclic deformation.

3.1.2 SME due to MT

The stress-strain curves and the strain-temperature curves in the case of maximum strain ε_m=6% are shown in Fig.3 and Fig.4, respectively. The curves are parametrized by the number of cycles N. As seen in Fig.3, yielding due to RPT occurs under stress of 60MPa in N=1, and yielding due to MT appears under

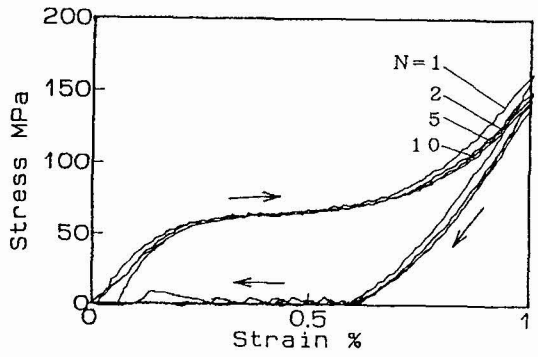

Fig.1 Stress-strain curves for SME due to RPT with thermomechanical cycles

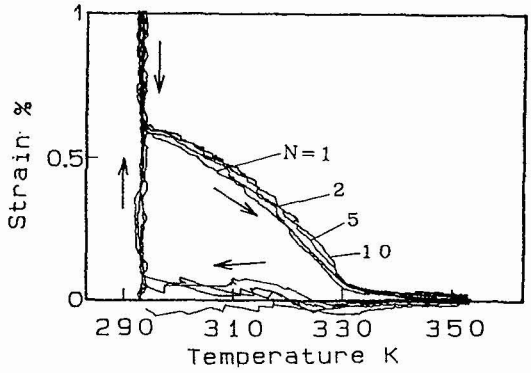

Fig.2 Strain-temperature curves for SME due to RPT with thermomechanical cycles

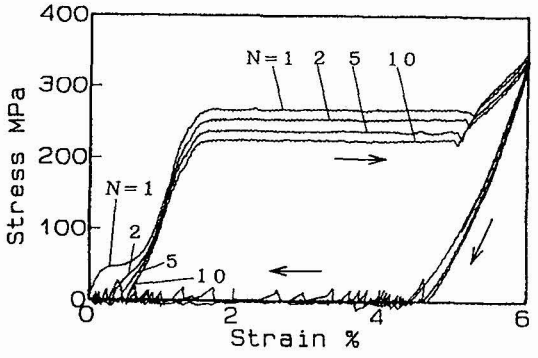

Fig.3 Stress-strain curves for SME due to MT with thermomechanical cycles

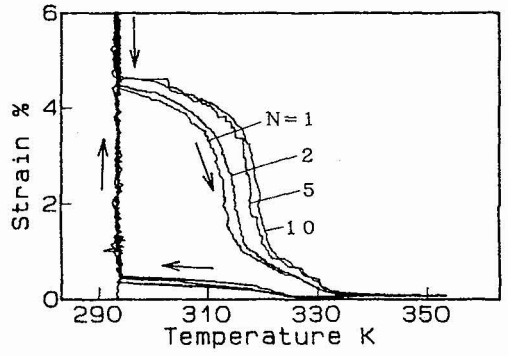

Fig.4 Strain-temperature curves for SME due to MT with thermomechanical cycles

stress of 280MPa in N=1. The MT stress decreases with an increase in N. The transformation strain induced in the loading process appears as residual strain after unloading and diminishes by heating under no stress, showing SME. As seen in Fig.4, strain recovers due to the MT reverse transformation at 315K in N=1 and recovers due to RPT thereafter in the heating process. The MT reverse transformation temperature increases with increasing N. In the cooling process under no stress, strain increases at the same temperature as the RPT reverse transformation temperature. The strain induced in the cooling process is called two-way strain which occurs due to the reversible SME. The two-way strain increases with increasing N and is 0.6% in N=10. Therefore the two-way strain is caused due to RPT.

The reason why these cyclic properties appear may be considered as follows. During the cyclic deformation, the interface between the parent phase and the R-phase or between the R-phase and the martensitic phase shifts repeatedly [14]. With cyclic movement of the interface, dislocations accumulate around the infinitesimal defects in the interface. Based on the increase in the dislocation density, internal stress increases [15]. Due to action of the internal stress, the MT stress decreases, the MT reverse transformation temperature increases and the two-way strain due to RPT increases with increasing N.

3.2 Superelasticity

3.2.1 SE due to RPT

The stress-strain curves with the loading-unloading cycles under ε_m=1% at temperature T=333K are shown in Fig.5. The curves are parametrized by the number of cycles N. As seen in Fig.5, the nonlinear

strain induced due to RPT in the loading process diminishes due to its reverse transformation in the unloading process, resulting in the hysteresis loop of SE. The width of the hysteresis loop is very narrow and the difference in stress between the loading curve and the unloading curve is smaller than 20MPa. The stress-strain curves vary little in N=1～20. Thus it is ascertained that the property of SE associated with RPT is stable for cyclic deformation.

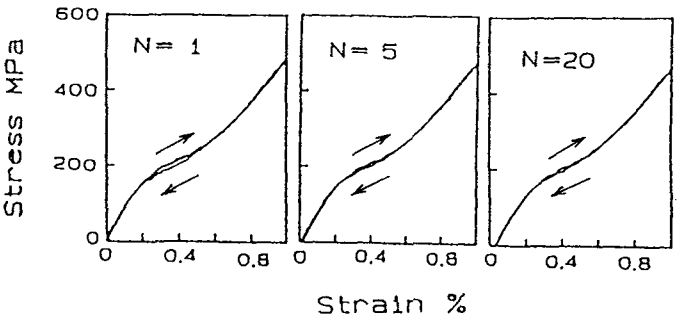

Fig.5 Stress-strain curves for SE due to RPT with loading-unloading cycles at constant temperature

3.2.2 SE due to MT

The stress-strain curves in the case of cyclic loading-unloading under constant maximum strain ε_m=8% at constant temperature T=353K are shown in Fig.6. The curves are parametrized by the number of cycles N. As seen in Fig.6, the MT stress σ_M and the reverse transformation stress σ_A decrease with the increase in N. Both transformation stresses decrease significantly in the early cycles and only slightly afterwards. The amount of decrease in σ_M with cycling is larger than that in σ_A. The residual strain which appears after unloading increases significantly in the early cycles and only slightly after these cycles. Therefore in order to obtain cyclic stability of SE in the application, the mechanical training before the practical use is necessary.

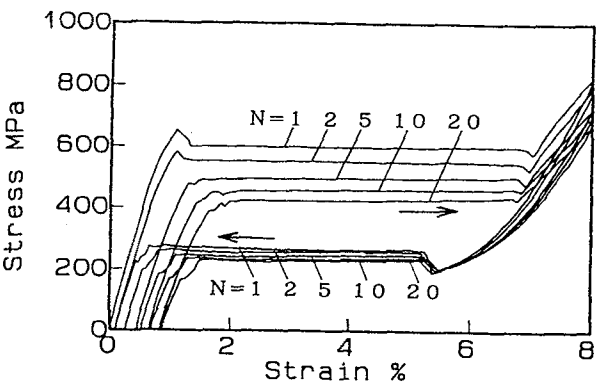

Fig.6 Stress-strain curves for SE due to MT with loading-unloading cycles at constant temperature

At the start point of MT, an overshoot of stress appears in the early cycles. This may occur due to the following reason. Because the externally applied load is removed completely in each cycle, all of the martensitic phase disappears in the unloading process. In order to induce MT in the reloading process, the creation of a nucleus of the martensitic phase is therefore necessary, leading to the observed overshoot of stress. The peak stress of overshooting is proportional to the magnitude of σ_M. The amount of overshooting decreases with increasing N.

On the other hand, an undershoot of stress occurs just before the reverse transformation sets in under constant stress σ_A in the unloading process. This is similar to the overshoot at the start point of MT in the loading process. At the point of ε_m=8% in the completion region of MT, the whole volume of the material consists of the martensitic phase. For the creation of a nucleus of the parent phase, it is necessary for the stress to decrease lower than the constant stress σ_A under which the reverse transformation progresses. Undershooting of stress therefore appears at the start point of the reverse transformation.

3.3 Transformation line

3.3.1 Stress-temperature phase diagram

The stress-temperature phase diagram of TiNi SMA is shown in Fig.7 [7]. In Fig.7, R, M, A and R'

represent the rhombohedral phase, martensitic phase, austenitic phase and rearranged rhombohedral phase, respectively. The parenthesized phase denotes the state obtained by unloading or by heating. The progress of the transformation is governed by the transformation kinetics. The starting and completing conditions of MT [16][17] and of RPT [18][19] are expressed by the linear functions of stress and temperature, respectively. These functions represent the boundaries between two phases in the stress-temperature phase diagram, which are called the transformation lines. In Fig.7, σ_M and σ_A denote the MT strip and its reverse transformation strip, and σ_M' and σ_A' the RPT strip and its reverse transformation strip, respectively. Each transformation strip is put in the starting line and the completing line of the corresponding transformation. The width of the RPT strip σ_M' is very narrow and the strip σ_M' is located between the MT strip σ_M and its reverse transformation strip σ_A. The RPT strip σ_M' almost overlaps its reverse transformation strip σ_A'.

3.3.2 MT line for cyclic deformation

The starting lines of MT σ_{Ms} and those of its reverse transformation σ_{As} in N=1 and 100 subjected to various thermomechanical paths are shown in Fig.8. These data were obtained by three kinds of experiments : (1) cyclic SME shown in Figs.3 and 4, (2) cyclic SE shown in Fig.6 and (3) cyclic recovery deformation due to heating-cooling under constant stress (Exp. RD). During cyclic deformation, the MT stress decreases and the MT temperature increases with increasing N. Therefore the MT lines move downward and to the right.

3.3.3 Transformation line for cyclic deformation

The cyclic behavior of the transformation lines of MT and RPT is schematically shown in Fig.9. In Fig.9, σ_{Ms}, σ_{Mf}, σ_{As} and σ_{Af} denote the starting lines and the completing lines of MT and its reverse transformation and σ_{Ms}', σ_{Mf}', σ_{As}' and σ_{Af}' the corresponding lines of RPT and its reverse transformation, respectively. Transformation lines in the first

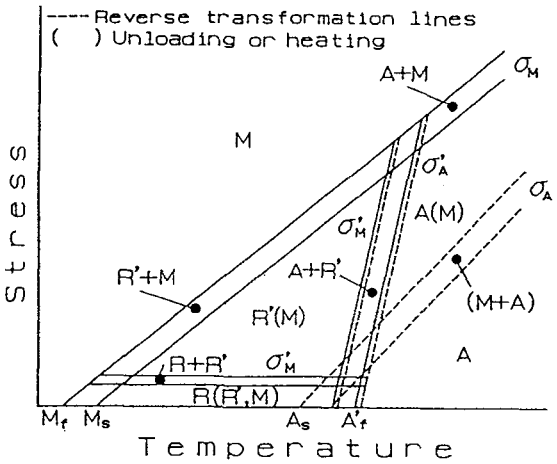

Fig.7 Stress-temperature phase diagram for MT and RPT

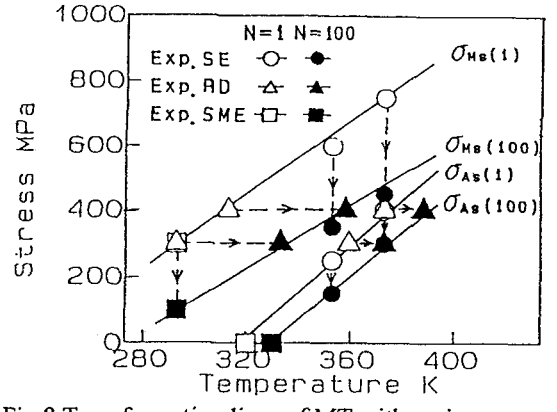

Fig.8 Transformation lines of MT with various thermomechanical paths in cycles N=1 and 100

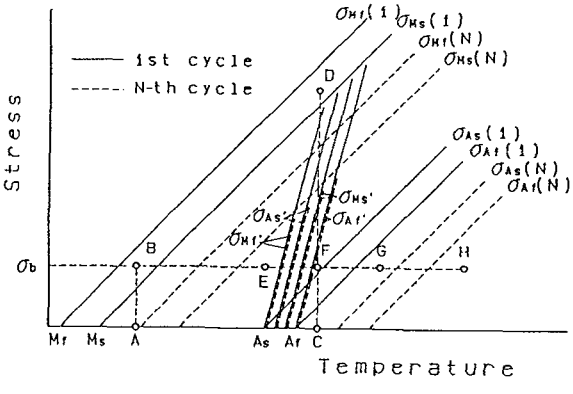

Fig.9 Schematic starting lines and completing lines of MT and RPT in first cycle and N-th cycle

cycle and N-th cycle are represented by a solid line and a dashed line, respectively.

Let us first consider the cyclic properties concerning MT. In the case that, after loading to the stress σ_b at the point B at T_A in which MT appears, a SMA element is heated with σ_b constant, if the temperature is raised above $\sigma_{Af}(1)$, for example, heated at the point G, the transformation strain recovers by the reverse transformation. If $\sigma_{Mf}(N)$ and $\sigma_{Af}(N)$ move to the right during the cyclic heating-cooling process with constant σ_b, the transformed strain does not recover upon heating at the point G. Then, to recover the transformed strain, it is necessary to raise the temperature at point H. MT is completed at T_A in the cooling process.

On the other hand, as shown in Fig.9, the RPT lines move little with thermomechanical cycles. In the case that a SMA element is operated under constant σ_b, although it is necessary for MT to heat and cool the element between points B and G, it is sufficient, for achieving RPT, to operate the element between points E and F. From this finding, it is ascertained that, because the difference in temperature to cause deformation associated with RPT is small, the response of the element with heating-cooling is fast. Thus it may be concluded that, for the element in which excellent cyclic property and fast response are important, RPT should be used. In this case, it should be taken into account that the RPT strain is smaller than 1%, which is smaller than one-tenth the MT strain.

3.4 Recovery Stress

3.4.1 Recovery stress under constant strain

The stress-temperature curves obtained in the cyclic heating-cooling tests are shown for each maximum strain ε_m in Fig.10. The relationships in N=1 and N=10 are shown. In the test after loading to ε_m and unloading at low temperature, residual strain appeared, and the heating-cooling process was repeated with holding the residual strain constant [11]. In Fig.10, the transformation lines of RPT and MT are shown by the dashed lines.

In the case of ε_m in the RPT region, stress increases or decreases remarkably along the RPT lines and is almost constant thereafter. The stress-temperature curves vary little with cycling.

In the case of ε_m in the MT region, stress increases in two stages during the heating process in N=1. That is, stress increases along the RPT reverse transformation line at first and along the MT reverse transformation line thereafter. The recovery stress increases in one stage in N=10. This phenomenon occurs because MT does not occur during the cooling process in N=1 and therefore only RPT and its reverse transformation occur repeatedly after the 2nd cycle.

The variation in the recovery stress from N=1 to 10 is smaller than 30MPa. The variation in the recovery stress is small considering that the MT stress subjected to thermomechanical cycling decreases by about 100MPa~200MPa in 10 cycles as observed in Figs.3 and 6. The recovery stress is thus stable for thermal cycling.

3.4.2 Recovery force of helical spring

The relationship between the axial force F_h at high temperature of the SMA coil subjected to the maximum deflection in hot water at 353K and the maximum shear strain γ_{max} on the surface of the coil is shown in Fig.11. The relationship between the recovery force effective for thermal cycling of the SMA coil F_r=F_h-F_l, which is determined by the difference between the axial force in hot water and the axial force in the air under the maximum deflection, and γ_{max} is also shown in Fig.11. In Fig.11, the solid curves are the results in the first cycle, and the dashed curves those in the 10^4th cycle.

As seen in Fig.11, the increase in F_h and F_r with γ_{max} decreases for $\gamma_{max} \geqq 2.5\%$, and both F_h and F_r decreases with increasing N. In the cross section of the wire of the coil, MT and RPT occur only in the surface area, and the state of the central part remains elastic [20]. It may be considered that, on the surface of the wire of the coil, RPT completes at γ_{max} =1.4% and MT starts at γ_{max} =2.1%. For $\gamma_{max} \geqq 2.5\%$, MT appears in the surface area of the wire, and both F_h and F_r decrease with increasing N. The amount of decrease in F_h and F_r at N=10^4 is somewhat smaller than that in σ_M observed in Figs.3 and 6. The recovery force does not vary in the RPT region. Thus, in the application of the SMA coils subject to cyclic

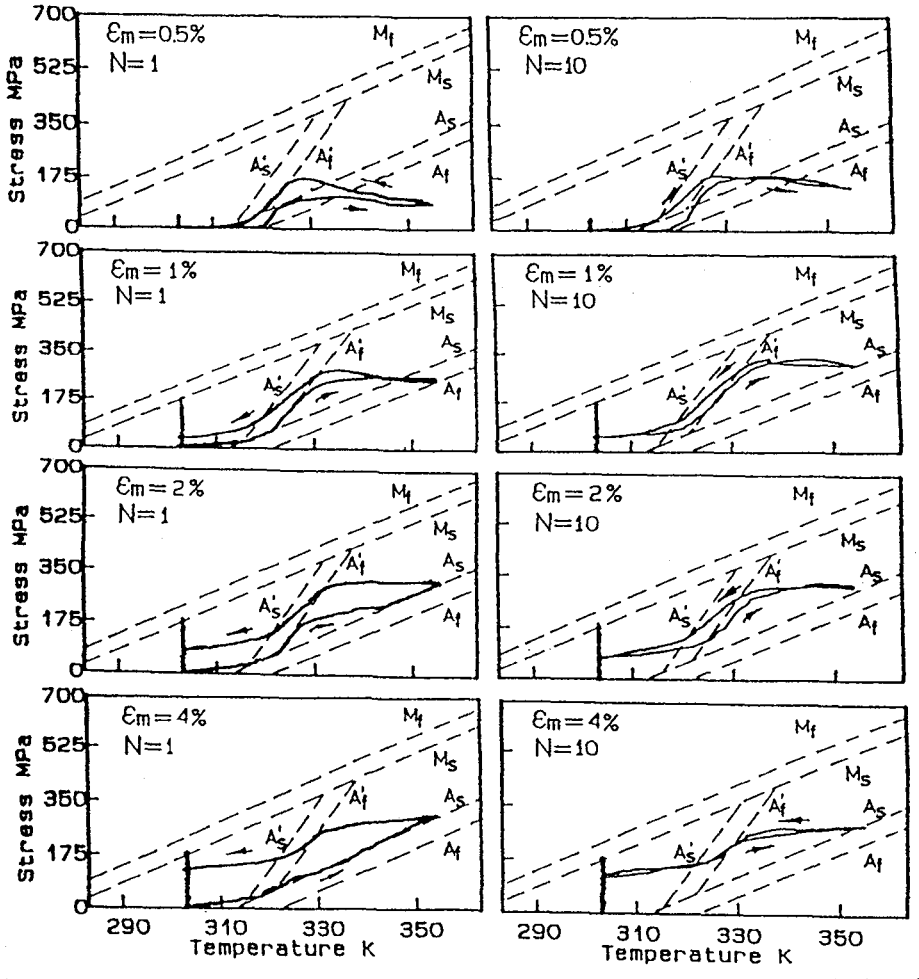

Fig.10 Stress-temperature curves with heating-cooling cycles under constant residual strain in cycles N=1 and 10

deformation, an almost constant recovery force is obtained.

3.5 Fatigue property

The relationship between the strain amplitude ε_a and the number of cycles to failure N_f obtained by the rotating-bending test at constant temperature T is shown in Fig.12. The strain amplitude ε_a is the maximum bending strain on the surface of a wire. When the wire is bent, RPT and MT expand from the surface area into the central part with increasing ε_a. Depending on ε_a, temperature increased by several degrees Kelvin during the rotating-bending cycles.

As seen in Fig.12, in the region of $\varepsilon_a \geqq 0.8\%$, N_f is small and decreases with increasing ε_a. Corresponding to Manson-Coffin relationship which is valid for normal metal in low-cycle fatigue, the relation between ε_a and N_f is expressed by a equation $\varepsilon_a = \alpha N_f^{-\beta}$. The value of β is 0.24 which is smaller than 0.5 which is valid for normal metal.

In the region of ε_a=0.8～1% or $N_f=10^4 \sim 10^5$, the strain-life curve has a knee. That is, if ε_a is in the RPT region of $\varepsilon_a \leqq 0.8\%$, N_f increases largely with decreasing ε_a and the curves approach the horizontal lines.

If the temperature T is high, the strain-life curves move to the left and downward with increasing T. That is, with respect to same ε_a, N_f decreases with increasing T. This phenomenon occurs due to the fact that the RPT stress and the MT stress increase with increasing T.

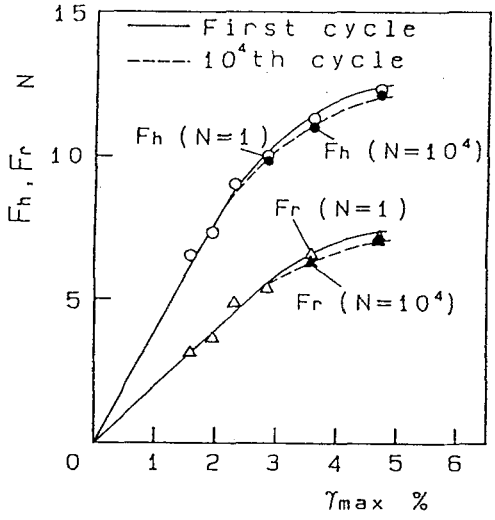

Fig.11 Dependence of axial force at high temperature and recovery force on maximum shear strain in first cycle and 10^4th cycle for helical spring

4. CONCLUSIONS

The thermomechanical properties of SME and SE due to MT and RPT of TiNi SMA are investigated experimentally by various loading-unloading and heating-cooling tests. The main results obtained are summarized as follows.

1. The MT stress decreases, the MT reverse transformation temperature increases and the MT line moves with increasing N. These characteristic properties due to MT vary significantly in the early cycles and only slightly afterwards.
2. The thermomechanical properties due to RPT vary little with cyclic deformation.
3. The recovery stress under constant strain and the recovery force of the helical spring are stable for thermomechanical cycling.
4. The rotating-bending fatigue life of the wire is quite long in the RPT strain region.

Acknowledgments

The experimental work in this study was carried out with the assistance of the students of Aichi Institute of Technology, to whom the authors wish to express their gratitude. The authors also wish to express their gratitude to Prof. K. Kimura and Prof. H. Iwanaga for their support, and to the Scientific Foundation of the Japanese Ministry of Education, Science and Culture for financial support.

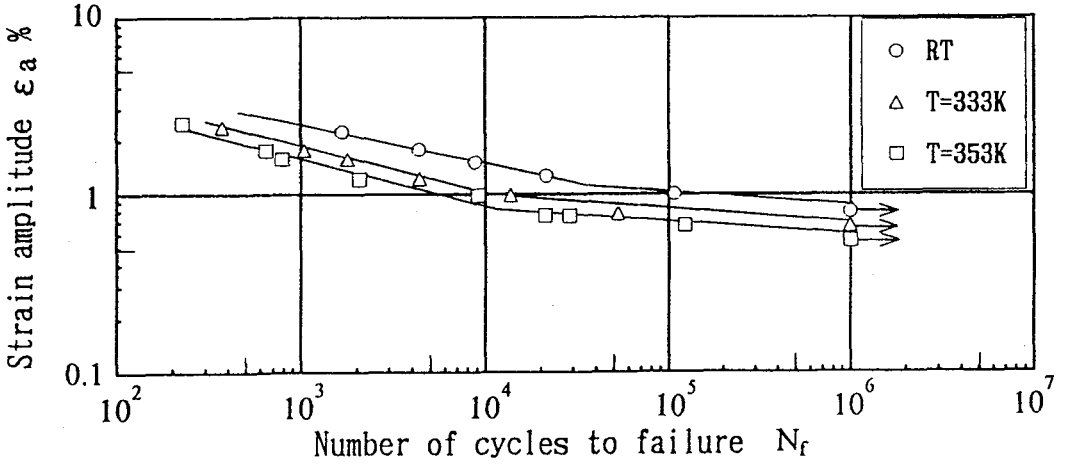

Fig.12 Strain-life curves for rotating-bending test at constant temperature T

References

[1] S. Miyazaki and K. Otsuka, *Phil. Mag.* A, **50**(1984), 393.
[2] S. Miyazaki and K. Otsuka, *Metall. Trans.* A(1986), 17A, 53-63.
[3] K. Otsuka, Engineering Aspects of Shape Memory Alloys ed. by T. W. Duerig, K. N. Melton, D. Stockel and C. M. Wayman, (1990), 36-45, Butterworth-Heinemann.
[4] H. Tobushi, H. Iwanaga, K. Tanaka, T. Hori and T. Sawada, *Continuum Mech. Thermodyn.*, **3**(1991), 79.
[5] J. L. McNichols, Jr. and P. C. Brookes, *J. Appl. Phys.*, **52**(1981), 7442.
[6] S. Miyazaki, Page 394 in Ref.[3].
[7] H. Tobushi, K. Tanaka, K. Kimura, T. Hori and T. Sawada, *JSME Inter. J.*, I, **35**-3(1992), 278-284.
[8] H. Tobushi, K. Kimura, H. Iwanaga and J. R. Cahoon, *JSME Inter. J.*, I, **33**-2(1990), 263-268.
[9] H. Tobushi, Y. Ohashi, A. Inaba, M. Kawaguchi and H. Sawada, *JSME Inter. J.*, I, **33**(1990), 256.
[10] H. Tobushi, K. Tanaka, T. Hori, T. Sawada and T. Hattori, *JSME Inter. J.*, A, **36**-3(1993), 314-318.
[11] P. H. Lin, H. Tobushi, K. Tanaka, C. Lexcellent and A. Ikai, *Arch. Mech.* **47**-2(1995), 281-293.
[12] H. Tobushi, Y. Ohashi, T. Hori and H. Yamamoto, *Exp. Mech.*, **32**-4(1992), 304.
[13] H. Tobushi, P. H. Lin, A. Ikai and S. Yamada, *Trans. of Jpn. Soc. Mech. Eng.*, A, **61**-591(1995), 2355-2361..
[14] H. Funakubo ed., Shape Memory Alloys, (1987), 39-60, Gordon and Breach Science Pub.
[15] S. Miyazaki, T. Imai, Y. Igo and K. Otsuka, *Metall. Trans.* A, 17A(1986), 115-120.
[16] K. Tanaka, S. Kobayashi and Y. Sato, *Inter. J. Plasticity*, **2**(1986), 59.
[17] K. Tanaka, T. Hayashi, Y. Itoh and H. Tobushi, *Mechanics of Materials*, **13**(1992), 207.
[18] T. Sawada, H. Tobushi, K. Kimura, T. Hattori, K. Tanaka and P. H. Lin, *JSME Inter. J.*, A, **36**-4(1993), 395-401.
[19] H. Tobushi, K. Kimura, T. Sawada, T. Hattori and P. H. Lin, *JSME Inter. J.*, A, **37**-2(1994), 138-142.
[20] H. Tobushi and K. Tanaka, *JSME Inter. J.*, I, **34**(1991), 83.